12-1-2014

Direct Synthesis of Methane from Co_2-H_2O Co-Electrolysis in Tubular Solid Oxide Electrolysis Cells

Long Chen

Fanglin Chen
University of South Carolina - Columbia, chenfa@cec.sc.edu

Changrong Xia

Publication Info

Published in *Energy & Environmental Science*, Volume 7, Issue 12, 2014, pages 4018-4022.

Chen, L., Chen, F., & Xia, C. (1 December 2014). Direct Synthesis of Methane from Co_2-H_2O Co-Electrolysis in Tubular Solid Oxide Electrolysis Cells. Energy & Environmental Science, 7 (12), 4018 – 4022. http://dx.doi.org/10.1039/C4EE02786H

Energy & Environmental Science

COMMUNICATION

View Article Online
View Journal | View Issue

Cite this: *Energy Environ. Sci.*, 2014, **7**, 4018

Received 2nd September 2014
Accepted 9th October 2014

DOI: 10.1039/c4ee02786h

www.rsc.org/ees

Direct synthesis of methane from CO_2–H_2O co-electrolysis in tubular solid oxide electrolysis cells†

Long Chen,[a] Fanglin Chen[b] and Changrong Xia*[a]

Directly converting CO_2 to hydrocarbons offers a potential route for carbon-neutral energy technologies. Here we report a novel design, integrating the high-temperature CO_2–H_2O co-electrolysis and low-temperature Fischer–Tropsch synthesis in a single tubular unit, for the direct synthesis of methane from CO_2 with a substantial yield of 11.84%.

Global advances in fossil-fuel-driven industrialization exacerbate various disquieting problems, particularly, increased scarcity of nonrenewable energy resources and heightened levels of atmospheric CO_2. Worldwide oil consumption has reached more than 90 million barrels per day, and still continues to increase at a considerable rate.[1] At the same time, burning fossil fuels emits a significant amount of greenhouse gas, and the concentration of atmospheric CO_2 has increased by 27% from 310 to 395 ppm during the past 60 years.[2] It has been widely accepted that the increased atmospheric CO_2 content is the major contributor to global warming and should be responsible for more and more intense weather phenomena and natural disasters. Consequently, alternative fuels and carbon-neutral energy technologies are indispensable in order to alleviate and potentially solve these energy and environmental problems. Co-electrolyzing CO_2 and steam using solid oxide electrolysis cells (SOECs) powered by renewable energy sources such as solar, wind, hydro, and geothermal heat is an efficient route for conversion of CO_2 into a syngas consisting of CO and H_2,[3–5] which can be further used to produce hydrocarbons with the Fischer–Tropsch (F–T) process.[6] Therefore, combining SOEC and F–T processes provides not only scalable energy storage means to solve the intermittency issues related to typical renewable power sources, but also an environmentally friendly solution to achieve quasi-carbon neutral fuel and chemical production with recycled CO_2. The combination is encouraged by nickel, which is the most widely applied electrocatalyst for SOECs[7] as well as the typical methanation catalyst for F–T synthesis. Methane, the main component of natural gas, has extensive industrial uses. Consequently, integrating the two processes in a single unit creates a novel strategy to convert CO_2–H_2O directly into methane.

However, there are technical challenges to effectively integrate the SOEC and F–T processes. High temperature (600–1000 °C) operation is preferred for SOECs due to favourable thermodynamics and kinetics considerations. The thermodynamic benefit is a decrease in the molar Gibbs energy of the reaction

Broader context

The rapid increase of the atmospheric concentration of carbon dioxide as a result of the extensive consumption of fossil fuels to meet the ever-increasing energy demand has led to serious environmental concerns worldwide. Thus, the efficient management and utilization of carbon dioxide is a paramount challenge. Co-electrolysis of steam and CO_2 in a solid oxide electrolysis cell (SOEC) is a promising solution to convert CO_2 to syngas, a mixture of H_2 and CO. It is also an effective storage medium for intermittent renewable energy sources such as wind, solar, and geothermal heat. Furthermore, syngas is an important feedstock for hydrocarbon synthesis through the Fischer–Tropsch (F–T) process. Consequently, by integrating the co-electrolysis with F–T synthesis in a single unit, a carbon neutral sustainable energy supply can be achieved. However, these two processes have very different optimal operating temperatures; SOECs prefer temperatures above 600 °C while F–T synthesis prefers below 350 °C. The substantial difference makes the integration very challenging. In this contribution, we present a novel design for direct synthesis of methane in a single tubular unit, demonstrating excellent integration of SOEC for CO_2–H_2O co-electrolysis at 800 °C and an F–T reactor for methanation at temperatures down to 250 °C.

[a]*CAS Key Laboratory of Materials for Energy Conversion, Department of Materials Science and Engineering & Collaborative Innovation Center of Suzhou Nano Science and Technology, University of Science and Technology of China, Hefei, Anhui 230026, China. E-mail: xiacr@ustc.edu.cn; Fax: +86 551 63601696; Tel: +86 551 63607475*

[b]*Department of Mechanical Engineering, University of South Carolina, Columbia, SC 29208, USA. E-mail: chenfa@cec.sc.edu; Fax: +1 803 7770106; Tel: +1 803 7774875*

† Electronic supplementary information (ESI) available: Fig. S1–S6, Schematic diagram for working principle of tubular unit, fabrication and characterization of tubular unit, data details for the unit operated under different models, impedance spectra and XPS analysis after 24 h short-term test. See DOI: 10.1039/c4ee02786h

with an increase of temperature while the molar enthalpy remains almost constant.[8] On the contrary, the F–T process of methanation is often conducted at low temperatures, typically 200–300 °C, to achieve high CH_4 yield since CO_x hydrogenation is strongly exothermic and thus thermodynamically favoured at reduced temperatures. Therefore, integrating the SOEC and F–T methanation, which are favoured in different temperature ranges in a single unit, has to compromise on the operation temperature. For example, 650 °C for the previously reported units.[9–11] Such temperature is selected to allow SOEC to be operated with reasonable efficiency to generate adequate syngas, but extremely impedes the methanation reaction. Consequently, only 0.2% CH_4 yield has been detected in a planar SOEC configuration of LSM–$Ce_{0.9}Gd_{0.1}O_{2-\delta}$/YSZ/$La_{0.2}Sr_{0.8}TiO_{3+\delta}$, where LSM is strontium doped lanthanum manganate, the electrocatalyst for the air electrode, YSZ is 8 mol% yttria stabilized zirconia, the electrolyte, and $La_{0.2}Sr_{0.8}TiO_{3+\delta}$ is the catalyst for the fuel electrode.[9] A similar yield of 0.286% is reported for a planar unit of LSM–ScSZ/ScSZ/Ni–ScSZ/Ni–YSZ, in which ScYZ is scandia stabilized zirconia, the electrolyte.[11] The CH_4 yield has to be substantially improved for practical applications.

Here, we show a new design of the direct synthesis of methane from CO_2–H_2O co-electrolysis using a tubular unit, which allows one part be controlled at high temperature for SOEC while the other at reduced temperature for F–T process (Fig. 1, see also S1 in ESI†). This design is capable of conducting various reactions including:

Reverse water gas shift (RWGS)

$$CO_2 + H_2 \rightarrow CO + H_2O$$

Co-electrolysis processes (SOEC)

$$2H_2O \rightarrow 2H_2 + O_2$$

$$2CO_2 \rightarrow 2CO + O_2$$

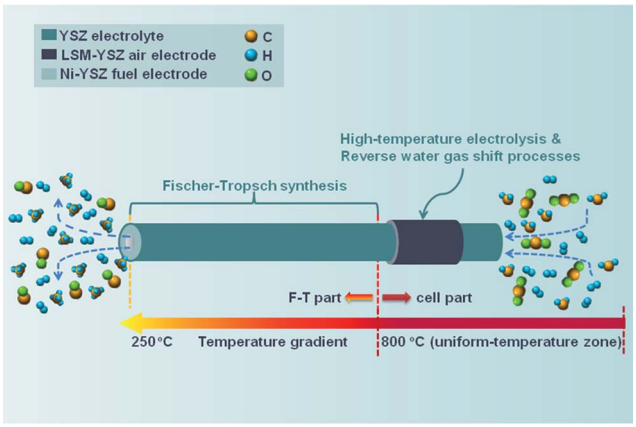

Fig. 1 Illustration of direct methane synthesis from CO_2–H_2O co-electrolysis in a tubular unit combining a high-temperature SOEC and a reduced temperature Fischer–Tropsch reactor.

And methanation

$$CO_2 + 4H_2 \rightarrow CH_4 + 2H_2O$$

$$CO + 3H_2 \rightarrow CH_4 + H_2O$$

The design is realized using a tubular porous Ni–YSZ substrate with a dense YSZ layer. As illustrated in Fig. 1, the cell part is operated at 800 °C while the electrolysis-induced syngas can be directly catalyzed to form methane in the F–T part at temperatures down to 250 °C. The design improves the CH_4 yield substantially to 11.84% as well as showing a stable 24 h short-term performance, demonstrating significant progress in the direct CO_2–H_2O conversion into hydrocarbon.

The schematic diagram and experimental details for the fabrication process of the tubular units are presented in Fig. S2 and S3.† Fig. 2a presents the cross-sectional microstructure of the cell part consisting of a 310 μm thick porous Ni–YSZ fuel electrode, a 12 μm dense YSZ electrolyte and a 30 μm porous LSM–YSZ air electrode. The electrolyte is dense and has intimate bonding with the electrodes. The fuel electrode near the electrolyte is porous with fairly uniform distribution of micro size solids and pores, which provides a large number of three-phase boundaries for the electrochemical reaction. The remaining portion of the Ni–YSZ fuel electrode beneath the active area is very porous with some finger-like pores and microvoids. The porosity is about 55%, high enough for facile gas transportation. The unique porous structure is formed by the modified phase inversion process, the mechanisms and details of which can be found in our previous work.[12]

The electrochemical performance is investigated in the fuel cell mode. Fig. 2b shows the performance when 20 mL min^{-1} humidified hydrogen is used as the fuel and air as the oxidant. Peak power densities of 0.48, 0.36 and 0.25 W cm^{-2} are obtained at 800, 750 and 700 °C, respectively. At 800 °C, the cell ohmic resistance is 0.36 Ω cm^2 while the total cell polarization resistance is 0.34 Ω cm^2. The cell performance is comparable with the typical tubular fuel cells prepared with the phase-inversion process.[12–14] The electrochemical performance is further investigated in the electrolysis mode at various steam concentrations using H_2 as the steam carrier (Fig. 2c). The cell voltage at zero current density denotes open-circuit voltage (V_{oc}), which decreases with the increase of the steam concentration as predicted from the Nernst equation. With an applied cell voltage of 1.5 V, a current density of 0.61 A cm^{-2} is observed for 20 vol% H_2O and increases to 0.83 A cm^{-2} for 50 vol% H_2O. Moreover, the current–voltage curves do not show any steam starvation phenomenon, demonstrating excellent gas transport property of the fuel electrode with the asymmetric porous microstructures (Fig. 2a and S4†). The corresponding hydrogen production rate is also presented in Fig. 2c. The hydrogen production rate increases with the electrolysis voltage and the humidity. For example, 3.16 mL min^{-1} cm^{-2} hydrogen can be achieved at 1.3 V and 40 vol% humidity.

Fig. 3a shows the results of CO_2–H_2O co-electrolysis. V_{oc} is slight lower than that for H_2O electrolysis (Fig. 2c), due to the

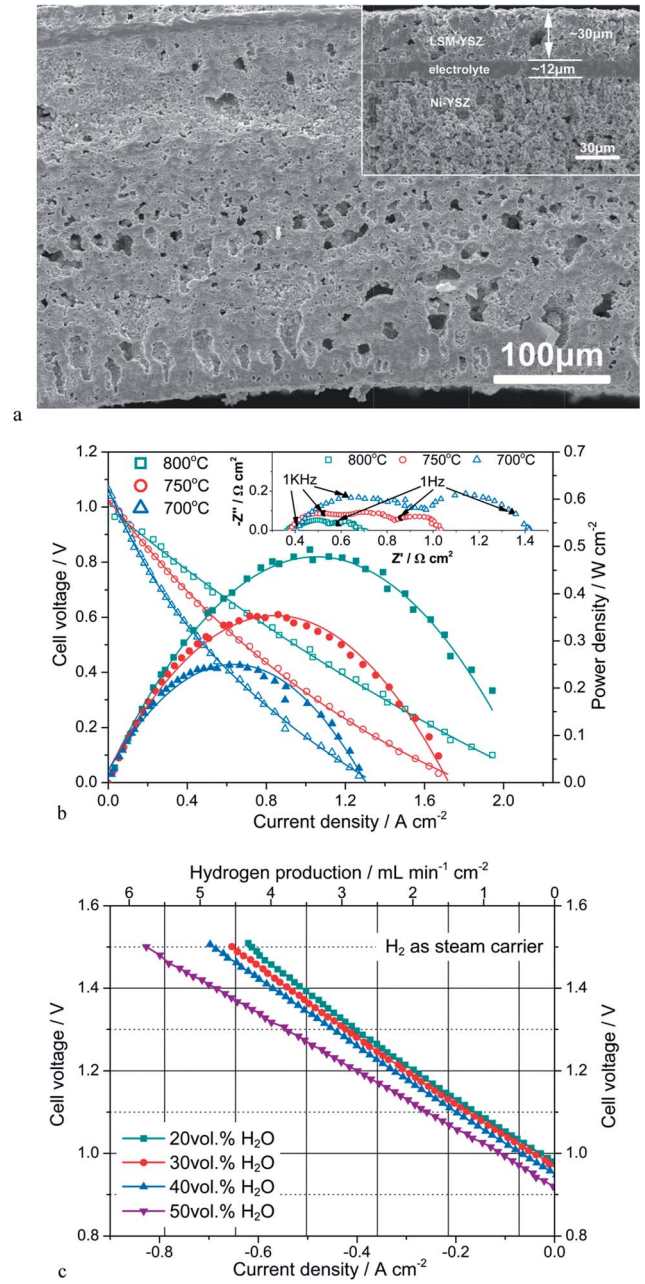

Fig. 2 Microstructures and performances for the LSM–YSZ/YSZ/Ni–YSZ tubular unit. (a) Cross-sectional SEM pictures of a tested cell. The up-right picture is the enlarged microview showing the electrode–electrolyte interfaces. (b) Cell voltage and power density as a function of current density in the fuel cell mode with 20 mL min^{-1} H_2 (2 vol% H_2O) as the fuel. The inset is the impedance spectra. (c) I–V curves and corresponding hydrogen production in the electrolysis mode obtained at different humidity and 800 °C using 20 mL min^{-1} H_2 as the steam carrier.

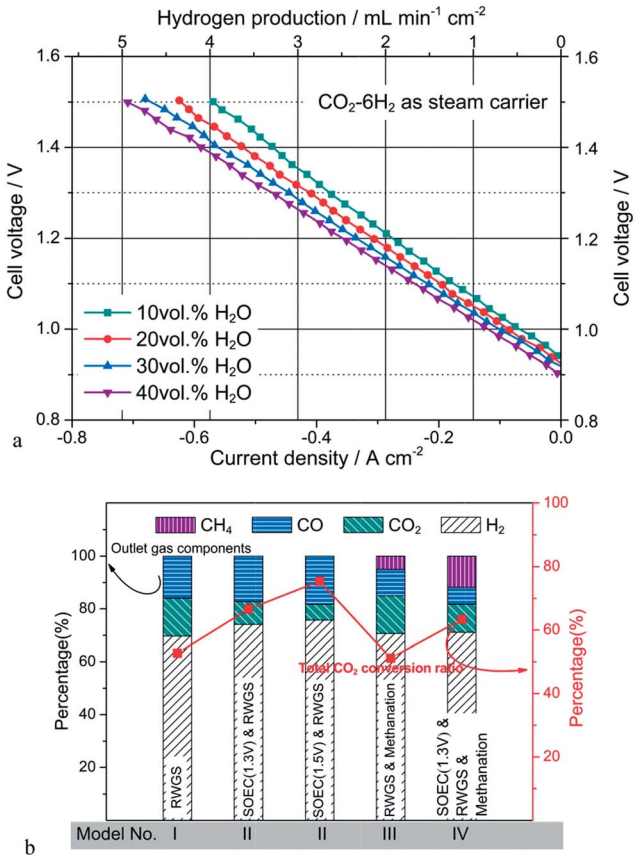

Fig. 3 (a) *I–V* curves and corresponding hydrogen production in the electrolysis mode obtained at different humidity and 800 °C using ~15 mL min^{-1} CO_2–H_2 (1 : 6, volume ratio) mixture as the steam carrier. (b) Component percentage in the outlet gas and total CO_2 conversion ratio under different operation conditions. Model I: Position A (ESI, Fig. S1,† the whole unit is subjected to 800 °C), V_{oc}, RWGS process only; Model II: Position A, external voltage applied, SOEC and RWGS processes; Model III; Position B (ESI, Fig. S1,† uniform 800 °C zone for SOEC part, 800–250 °C temperature gradient for F–T part), V_{oc}, RWGS and methanation processes; Model IV: Position B, 1.3 V external voltage, SOEC, RWGS and methanation processes. The inlet gas is ~15 mL min^{-1} CO_2–H_2 (1 : 6, volume ratio) mixture with 20 vol% humidity.

increased oxygen partial pressure by CO_2. The co-electrolysis performance is very close to the H_2O electrolysis. For example, at 1.3 V and 40% humidity, the current density is 0.47 and 0.45 A cm^{-2} for the CO_2–H_2O (Fig. 3a) and H_2O (Fig. 2c), respectively. Previous research has reported that CO_2–H_2O co-electrolysis is dominated by steam reduction to hydrogen whereas CO_2 is reduced to CO by the reverse water gas shift (RWGS) reaction.[15] Assuming 100% current efficiency for steam reduction, 3.24 mL min^{-1} cm^{-2} hydrogen can be achieved at 1.3 V and 40 vol% humidity.

The tubular unit can be used to conduct the SOEC, methanation and RWGS reactions using Ni as the catalyst (Fig. 3b). When the unit is in Position A (ESI, Fig. S1†), the F–T part and cell part are at the same temperature of 800 °C, which is favoured for the RWGS reaction but too high for the methanation. Under the open circuit conditions, only RWGS takes place (Model I), producing CO (15.98%) from the feeding CO_2–H_2 mixture. When the unit is under an external electrical field, both RWGS and SOEC are active (Model II). CO production is increased to 17.24% and 18.31% at 1.3 V and 1.5 V, respectively. As mentioned above, the improved CO production is mainly produced from the RWGS reaction through promoted H_2 concentration from the electrolysis process. The total CO_2

conversion ratio is increased by the electrolysis process from 52.7% for Model I to 66.6 and 75.4% for the Model II at 1.3 V and 1.5 V, respectively. However, no CH_4 component can be detected when the unit is in Position A, demonstrating that the methanation reaction cannot proceed at 800 °C. When it is put at Position B (ESI, Fig. S1†), the tubular unit is in a non-uniform temperature field. The cell part is at 800 °C while the F–T part is subject to temperature gradient from 800 to 250 °C. The reduced temperatures are favoured for methanation, and CH_4 (5.02%) is obtained at V_{oc} (Model III). Much more CH_4 is produced when an external electrical field is applied (Model IV). The CH_4 yield is 11.84% at 1.3 V, significantly higher than those reported using planar SOECs at a cell temperature of 650 °C, in which the CH_4 yield is only 0.2–0.3%.[9,11] The 11.84% yield means 41.0% of CO_2 is converted to CH_4 through Model IV. It should be noted that a high mechanical stability is expected in Position B although a temperature gradient is applied to the F–T part, where the porous Ni–YSZ and dense YSZ have well matched thermal expansion coefficients.

For the methanation process, the increased CO and H_2 concentrations and decreased H_2O concentration are kinetically favourable. On the other hand, the reduced temperatures are thermodynamically favourable due to the exothermic process of hydrogenation. Therefore, a remarkable CH_4 yield is achieved using the unique design that integrates the two functional chambers in a single tubular unit. This unique design allows the SOEC chamber to operate at 800 °C to increase the H_2 concentration and decrease the steam partial pressure. Furthermore, high temperature can improve the electrolysis kinetics as well. Meanwhile, the methanation chamber at reduced temperatures is thermodynamically favourable for CH_4 formation. Moreover, the temperature control can be easily realized with a mini-mite furnace (ESI, Fig. S1†). For scaling up test, the exhausted heat could be used to preheat the inlet CO_2–H_2O to achieve the thermal integration.

Fig. 4 presents the short-term performance of the tubular unit operated in Model IV (for details see Table S1, ESI†). Fig. 4a shows that the current density decreases slightly at first and then is stabilized at 0.42 A cm^{-2} with the elapsed time. Moreover, both CH_4 and CO show a stable yield during the test. The average CH_4 yield is 11.40% (0.84 mL min^{-1}) with the total CO_2 conversion ratio of 64.1%. The post tested impedance spectra and X-ray photoelectron spectroscopy also confirm the stable performance under Model IV operating conditions (ESI, Fig. S5 and S6†). Moreover, the by-product (CO–H_2 syngas) is also highly valuable and can be further cycled to improve methane yield. Higher hydrocarbons yield may be obtained by further improving the F–T synthesis conditions, such as employing high-efficiency methanation catalysts.

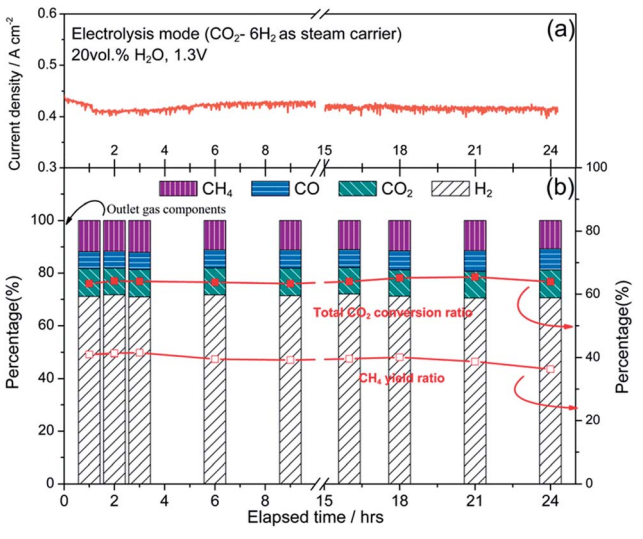

Fig. 4 Performance of a tubular unit operated in Model IV at 1.3 V. The inlet steam carrier is ~15 mL min^{-1} CO_2–H_2 (1 : 6, volume ratio) with relative humidity of 20%. (a) Current density; (b) outlet gas components, total CO_2 conversion ratio and CH_4 yield ratio *versus* elapsed time.

Conclusions

In this work, we have demonstrated a tubular design for direct synthesis of CH_4 from CO_2–H_2O feedstock. This unique design substantially improves CH_4 yield to 11.84% by combining the CO_2–H_2O co-electrolysis and methanation in a single tubular unit. 24 h short-term test shows that the co-electrolysis process presents a generally stable current density at 0.42 A cm^{-2} during the electrolysis operation while the average CH_4 yield can reach 11.40% (0.84 mL min^{-1}) with an overall CO_2 conversion ratio of 64.1%. The novel integration of CO_2–H_2O co-electrolysis and methanation in a single tubular unit presents a significant advancement in hydrogen economy and a carbon neutral renewable energy cycle.

Acknowledgements

We greatly appreciate supports from the National Natural Science Foundation of China (51372239), the Ministry of Science and Technology of China (2012CB215403) and the U.S. National Science Foundation (DMR-1210792).

Notes and references

1 U. S. E. I. A. (EIA), Short-term Energy Outlook, http://www.eia.gov/forecasts/steo/index.cfm, accessed 12 August 2014.
2 M. McGee, 399.00ppm: Atmospheric CO_2 for July 2014, http://co2now.org/, accessed 6 August 2014.
3 Q. X. Fu, C. Mabilat, M. Zahid, A. Brisse and L. Gautier, *Energy Environ. Sci.*, 2010, **3**, 1382–1397.
4 C. Graves, S. D. Ebbesen, M. Mogensen and K. S. Lackner, *Renewable Sustainable Energy Rev.*, 2011, **15**, 1–23.
5 K. Christopher and R. Dimitrios, *Energy Environ. Sci.*, 2012, **5**, 6640–6651.
6 G. P. Van Der Laan and A. A. C. M. Beenackers, *Catal. Rev.: Sci. Eng.*, 1999, **41**, 255–318.
7 T. Ishihara, N. Jirathiwathanakul and H. Zhong, *Energy Environ. Sci.*, 2010, **3**, 665–672.

8 L. Bi, S. Boulfrad and E. Traversa, *Chem. Soc. Rev.*, 2014, DOI: 10.1039/c4cs00194j.
9 K. Xie, Y. Q. Zhang, G. Y. Meng and J. T. S. Irvine, *Energy Environ. Sci.*, 2011, **4**, 2218–2222.
10 K. Xie, Y. Q. Zhang, G. Y. Meng and J. T. S. Irvine, *J. Mater. Chem.*, 2011, **21**, 195–198.
11 W. Y. Li, H. J. Wang, Y. X. Shi and N. S. Cai, *Int. J. Hydrogen Energy*, 2013, **38**, 11104–11109.
12 L. Chen, M. T. Yao and C. R. Xia, *Electrochem. Commun.*, 2014, **38**, 114–116.
13 C. L. Yang, W. Li, S. Q. Zhang, L. Bi, R. R. Peng, C. S. Chen and W. Liu, *J. Power Sources*, 2009, **187**, 90–92.
14 C. H. Yang, C. Jin and F. L. Chen, *Electrochim. Acta*, 2010, **56**, 80–84.
15 Z. L. Zhan and L. Zhao, *J. Power Sources*, 2010, **195**, 7250–7254.